EJGO European Journal of Gynaecological Oncology

Intraoperative molecular imaging can identify sub-centimeter peritoneal implants during ovarian cancer cytoreductive surgery

J.L. Tanyi[1,6], L. Cory[1], E. DeJesus[2], J. Keating[2,6], J. Predina[2], S. Nie[4], C. Deshpande[3], P. Low[5], S. Singhal[2,6]

[1] Department of Obstetrics and Gynecology, [2] Department of Surgery, [3] Department of Pathology, University of Pennsylvania Perelman School of Medicine, Philadelphia, PA

[4] Departments of Biomedical Engineering and Chemistry, Emory University, Atlanta, GA

[5] Department of Chemistry, Purdue University, West Lafayette, IN

[6] Center for Precision Surgery, Abramson Cancer Center, University of Pennsylvania Perelman School of Medicine, Philadelphia, PA (USA)

Summary

Objective: To investigate the impact of fluorescent imaging on intraoperative identification of sub-centimeter tumor implants as a means of improving detection and removal of cancer deposits. *Materials and Methods:* In order to confirm the distribution of the folate receptor alpha (FRα), sections of 20 ovarian tumors and seven normal ovarian tissues were obtained and immunohistochemistry was performed using monoclonal antibody mAb343 to evaluate FRα expression. To investigate the value of fluorescent imaging in vivo in ovarian cancer surgery, an animal xenograft model was used. NOD/SCID/Gama mice were subcutaneously or intra-peritoneally injected with IGROV-1, SKOV3, KB cells, and IOSE cells. Surgical evaluation of the tumor infiltrated area was done after the folate-FITC conjugate infusion. The surgeon's visual inspection and palpitation was used first and thereafter fluorescence imaging was applied to determine if additional nodules could be located. In addition, for further in vivo evaluation, five human patients with ovarian cancer were systemically infused with 0.1 mg/kg of the folate-FITC conjugate four hours prior to cytoreductive surgery. During the standard of care operation, the surgeons performed the standard approach and inspected the body cavity for tumor nodules using unaided visual inspection and palpation followed by examination with fluorescence imaging. The authors analyzed the tumor background ratio (TBR) to tumor size for each nodule. *Results:* Seventeen out of 20 tumors displayed moderate (2+) to strong (3+) expression of FRα with no staining of surrounding stroma. Using fluorescence microscopy, fluorescent dye uptake was seen uniformly on IGROV-1 and SKOV-3 cell lines and the intensity peaked at one hour and localized to the cell surface with cytosolic staining. By Day 14, the surgeon, without intraoperative imaging, identified an average of seven nodules per animal (range 0-12), whereas the surgeon could identify a mean of 11 nodules (range 0-18, $p < 0.03$) with intraoperative imaging. In triplicate experiments, the addition of the intraoperative imaging allowed investigators to locate one to five more nodules per mouse (mean 3.8, $p < 0.01$). The peak TBR in the primary tumor to normal tissue was at four hours. At that time point, the TBR was 23.6 ± 8.7. In human evaluation, no toxicity was detected. *Conclusions:* Intraoperative fluorescent imaging of FRα positive ovarian cancer increased the removal of residual disease in murine model effectively during debulking surgery. The application of the technology in human requires future human studies.

Key words: Ovarian carcinoma; Folate receptor; Fluorescence imaging; Cytoreduction; Molecular imaging.

Introduction

It is estimated that more than 22,000 women will be diagnosed with ovarian cancer in the United States during 2016 [1]. Surgical cytoreduction plays an important role in the management of these women, and the single most important prognostic indicator is a complete surgical debulking of all disease [2]. Although bulky disease can be easily recognized with the unaided eye during surgery, sub-centimeter implants are often difficult to discriminate from adjacent normal tissues such as pelvic fat, omentum, and epiploica of large bowels. Thus, the risk of recurrent disease is markedly increased in patients with sub-centimeter peritoneal implants. The present authors hypothesized that if sub-centimeter implants could be visually enhanced intraoperatively, these cancerous tissues would more easily be identified and this would result in superior disease clearance.

The present group and others have studied intraoperative tumor imaging and identification, utilizing targeted and non-targeted therapies [3-8]. The underlying premise is that tumor fluorescence would allow surgeons to improve detection of cancer deposits intra-operatively. Currently, multiple technologies exist that allow tumor cells to fluoresce in rodent models, but there has been limited success in humans. Development of similar techniques in humans has been hampered due to the limited ability of visible light to excite fluorophores through thicker tissues of humans, toxicity, and paucity of clinically approved probes.

In order to target ovarian adenocarcinomas with a fluorophore, the present authors selected the folate receptor

Revised manuscript accepted for publication October 5, 2016

alpha (FRα), encoded by the FOLR1 gene, because it is an attractive molecular candidate for epithelial ovarian carcinomas [9-12]. FRα is a 40 kD glycosylphosphatidyl-inositol-linked protein that is overexpressed by 10- to 100-fold in ovarian malignancies compared to normal cells and it increases in concentration with tumor progression [13-15]. Folate is an essential vitamin required for DNA synthesis in both normal and tumor cells, and it may confer a growth advantage to the ovarian tumors by modulating folate uptake from serum. Ovarian tumors have been shown in other studies to highly express FRα [12]. Also, the receptor expression is unaltered after chemotherapy, so it is a robust, reliable target for molecular imaging [12]. The goal of this study was to evaluate FRα as a target for intraoperative imaging of sub-centimeter ovarian tumors. A recent report in humans utilized a folate-fluorescein conjugate specific to ovarian tumors thereby showing clinical feasibility [8]. The present authors chose to further evaluate this approach, specifically focusing on sub-centimeter ovarian tumor nodules.

Materials and Methods

The cell lines IGROV-1 and SKOV-3 were kind gifts from Gordon B. Mills, MD. IGROV-1 is an ovarian carcinoma of a 47-year-old woman that was established in tissue culture and in nude mice [16]. SKOV-3 is a ovarian carcinoma cell line from a 64-year-old Caucasian female also established in tissue culture. The cells were cultured in modified Roswell Park Memorial Institute (RPMI) medium supplemented with penicillin/streptomycin, glutamine and 10% fetal bovine serum and deficient in folate. Cultures were incubated at 37°C in humidified air with 5% CO_2 and regularly tested and maintained negative for *Mycoplasma spp*. Formalin-fixed, paraffin-embedded (FFPE) tumor blocks from ovarian cancer patient samples were obtained under an IRB-approved tumor collection protocol of University of Pennsylvania. Originally the tumor samples from patients diagnosed with primary epithelial ovarian carcinoma were included in this analysis, which was performed with IRB approval from previously untreated patients undergoing debulking surgery. All specimens were processed in compliance with IRB of University of Pennsylvania and the Health Insurance Portability and Accountability Act (HIPAA) requirements. Formalin-fixed, paraffin-embedded human tissue samples available from surgery or biopsy were analyzed for FR by an immunohistochemistry assay specific for the α-isoform of FR. Evaluation of the stained samples was accomplished in a semi-quantitative manner with light microscopy to assess the degree of circumferential membranous staining in the tumor cell population.

Folate-fluorescein isothiocyanate (folate-FITC) is a conjugate between folate and fluorescein isothiocyanate. This conjugate forms a negatively charged fluorescent molecule that binds weakly and non-specifically to serum proteins at a level of ~75%. FITC is a synthetic organic compound that is excited in the 465-490 nm wavelength and emits light in the 520-530 nm range (visible spectrum). A 0.1 mg/kg dose of this agent was dissolved in 10 milliliters of normal saline, and then given to patients via peripheral vein injection four hours prior to the operation.

Intraoperative imaging was performed using a fluorescence imaging system, FloCam, or a prototype system developed in the authors' laboratory [6]. Positive and negative controls were used for all images. In order to quantitate the tissue fluorescence, the authors used region-of-interest software and HeatMap plugin within ImageJ (http://rsb.info.nih.gov/ij/; public domain free software developed by National Institutes of Health). A background reading was taken from adjacent normal tissue in order to generate a tumor-to-background ratio (TBR).

All protocols employed in this study were approved by the University of Pennsylvania Institutional Animal Care and Use Committee. Mice were injected subcutaneously on the flanks of NOD/SCID/Gama mice with 2.0×10^6 IGROV-1, SKOV3, or 1.5×10^6 IOSE cells. Tumor cells for subcutaneous injections were suspended in 100 μL PBS. Tumor volume was calculated using the formula (3.14 × long-axis × short-axis^2)/6. Mice were fed an exclusively folate deficient chow on the day of inoculation until imaging. Surgery was performed on mice bearing flank tumors using an established resection model [17]. Surgery was performed when tumors reached ~300 mm^3. Mice were anesthetized with intramuscular ketamine (80 mg/kg) and xylazine (10 mg/kg), shaved, and the surgical field sterilized prior to surgery. A 1- to 2-cm incision was made adjacent to the tumor and it was removed using standard blunt and sharp dissection techniques. After imaging, the incision was closed using sterile silk 4-0 sutures. Buprenorphine (0.2 mg/kg) was administered at the time of surgery and six hours postoperatively to provide analgesia.

An additional 40 animals [IGROV-1 (n=20) and SKOV-3 (n=20)] were used to establish an intraperitoneal model of metastasis in six-week old female mice. Mice were again maintained on folate-deficient chow from the time of inoculation to time of imaging. NOG/SCID mice were injected with IGROV-1 cells in their abdomen on Day 0. After a seven-day incubation period, five mice a day every other day were euthanized and their abdomens explored for two weeks (Days 8 to Day 21). Two investigators counted the total number of implants by visual inspection alone. Each implant was removed and then stored in formalin for future histology. Then, intraoperative imaging with the imaging device and fluorescence was performed to locate any additional nodules that may have been unrecognized by the unaided eye. Suspicion for a tumor was defined as any nodule that had a TBR >1.5. Each nodule was excised and placed in formalin for H&E. Final pathology served as the gold standard for identifying a tumor nodule.

All patients underwent informed consent approved by the

University of Pennsylvania IRB. Any patient with recurrent ovarian cancer who was deemed a surgical candidate was eligible for this study and underwent CT scanning before the surgery. The patients were specifically consented for the possibility that additional tissue may be resected based on findings from intraoperative tissue fluorescence, although the magnitude of the operation would not be significantly altered. A standard-of-care operation was performed on each patient and was not significantly altered for purposes of this study. The sequence of the operation was as follows. Four hours prior to surgery, patients were systemically infused with 0.1 mg/kg of the folate-FITC conjugate. Vital signs were obtained every five minutes following injection for 60 minutes after injection. Adverse events were monitored through the time of the patient's follow-up laboratory measurements at 12 and 24 hours after injection. Additionally, the patients were instructed to report any adverse events that occurred up to one month after injection.

During the operation, the surgeons performed the standard incision and inspected the body cavity for tumor nodules using unaided visual inspection and palpation. When nodules were identified, the operating room lights were dimmed and the nodule was examined for fluorescence. The nodule was photo-documented both by white light and fluorescence. Next, the planned cancer resection was performed. Following removal of the tumor, the specimens were again examined ex vivo for tumor fluorescence before sending them to pathology. Once the planned cytoreductive surgery was felt to be complete, the lights were dimmed for a second time and the open body cavity was inspected for residual fluorescent cancer cells in tumor deposits anywhere in the operative field or at the margins of the resection. Frozen section biopsies were performed when indicated. All specimens were sent for permanent histopathology.

Prior studies have shown that FRα is expressed on ovarian cell carcinomas [11, 14, 18]. On normal ovarian tissues, FRα is expressed on the apical surface of oviduct epithelial cells [13]. In order to confirm the distribution of the receptor on these tissues, sections of 20 tumors and seven normal ovarian tissues were obtained from the operating room. Formalin-fixed, paraffin-embedded samples were stained for FRα with monoclonal antibody mAb343 (1.8 mg/ml) by standard protocols previously described [5]. FRα membrane staining intensities were scored as 0 (no staining), 1+ (weak), 2+ (moderate), and 3+ (strong). Scores were averaged for three high powered fields from the same tumor specimen. An average score of 0 was classified as no expression, 1 was classified as weak expression, and 2 or 3 were classified as strong expression. To detect FITC, the monoclonal antibody Mab10257 was used following cell membrane permeabilization with methanol. Lastly, a biopsy of each tumor was frozen-sectioned and imaged using fluorescence microscopy. Fluorescence microscopy

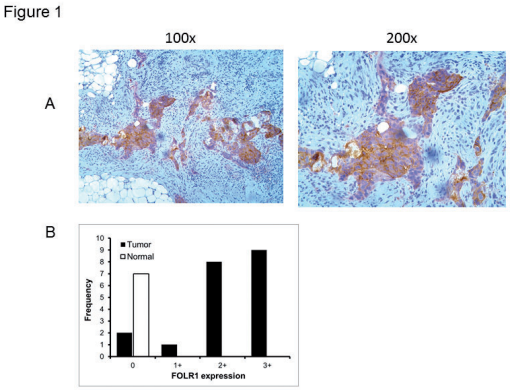

Figure 1. — Immunohistochemical staining of FRα in human ovarian adenocarcinomas.
Immunohistochemical staining of human adenocarcinomas showed that ovarian epithelial tumors strongly express FRα. A) IHC of a typical ovarian tumor at ×100 and ×200. B) In 20 patients, 17 ovarian tumors were 2^+ to 3^+ in expressing FRα. Normal ovarian epithelial cells did not express the receptor.

was performed using an fluorescent microscope equipped with a FITC-specific filter set. Data from fluorescence microscopy were compared to the subjective and quantitative measurements of fluorescence.

The authors assessed the significance of differences in median values (size, TBR) of non-fluorescing *vs.* fluorescing tumors by the Mann-Whitney test. They tested for differences in paired samples using the Wilcoxon signed-rank test, assessed correlation of continuous outcomes by the Pearson correlation coefficient, and conducted all analyses in SAS Version 9.3.

Results

The authors found that 17 out of 20 tumors displayed moderate (2^+) to strong (3^+) expression of FRα with no staining of surrounding stroma and immune cells (Figure 1). There was weak to no expression in three cases, both of which were confirmed to be serous ovarian adenocarcinomas. There was no correlation between stage and grade with FRα expression ($p > 0.2$). All of the normal ovarian tissues had weak to no FRα expression.

Next, in order to identify ovarian cancer cell lines that may express FRα, two, well-established human ovarian carcinoma cell lines (IGROV-1 and SKOV-3) and an immortalized ovarian epithelial cell line (IOSE) were selected for immunohistochemistry. Immunostaining with a FRα monoclonal antibody demonstrated both carcinoma cell lines avidly expressed FRα, whereas the control cell line did not express this surface receptor (Figure 2).

To demonstrate that the folate-fluorophore conjugate

Figure 2a

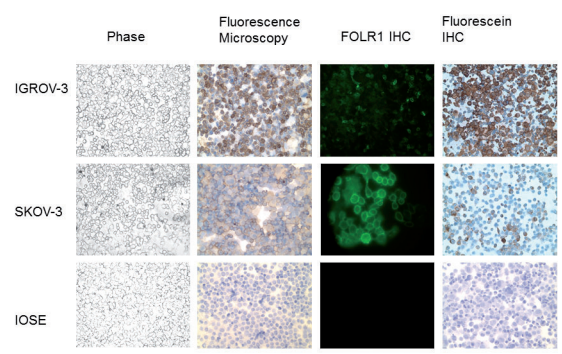

Figure 2b

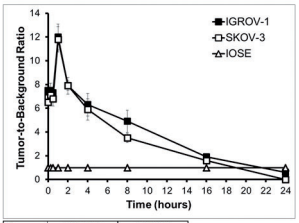

Time	IGROV-1	SKOV-3
0 min	6.90 ± 0.55	6.60 ± 0.59
5 min	7.20 ± 0.36	6.50 ± 0.52
15 min	6.60 ± 0.59	7.20 ± 0.36
30 min	6.70 ± 0.40	6.70 ± 0.54
1 hour	10.60 ± 0.64	13.80 ± 1.24
2 hours	7.60 ± 0.61	9.50 ± 0.67
4 hours	6.50 ± 0.78	6.20 ± 0.87
8 hours	4.90 ± 0.59	3.70 ± 0.56
16 hours	1.90 ± 0.34	1.70 ± 0.34
24 hours	0.10 ± 0.02	0.80 ± 0.10

Figure 2. — Folate-fluorescein detection in murine and human cell lines.
IGROV-1 and SKOV3 cell lines displayed positive FOLR1immunohistochemical staining. A) Folate-fluorescein staining of IGROV-1 and SKOV-3 cell lines showed positive staining confirmed by fluorescence microscopy and anti-FITC immunohistochemical staining. The negative control, IOSE, showed no expression of FRα. B) In vitro studies showed maximal tumor fluorescence within one hour and the loss of all signal by 24 hours.

could act as specific ligand for tumor cells, the authors tested it on IGROV-1 and SKOV3. IOSE served as the background control. The folate-fluorescein conjugate was co-incubated with each cell line for one hour at five different concentrations: 0.1 uM, 0.01 uM, 0.001 uM, 0.0005 uM, and 0.0001 uM. After removing free dye by PBS washing, the stained cells were imaged using fluorescence microscopy at varying intervals. Tumor cells were kept in a dark chamber between imaging, and all experiments were repeated in triplicate. Dye uptake was seen uniformly on IGROV-1 and SKOV-3 (Figure 2). The fluorescent intensity peaked at one hour and localized to the cell surface with cytosolic staining. For IGROV-1, the peak TBR at 0.1 uM, 0.01 uM, 0.001 uM, 0.0005 uM, and 0.0001 uM concentration at one hour was 18.1 ± 3.3, 16.6 ± 5.3, 5.4 ± 1.3, 1.5 ± 1.7, and 1.3 ± 0.8, respectively. By 24 hours, the fluorescence was undetectable in all cases.

Figure 3

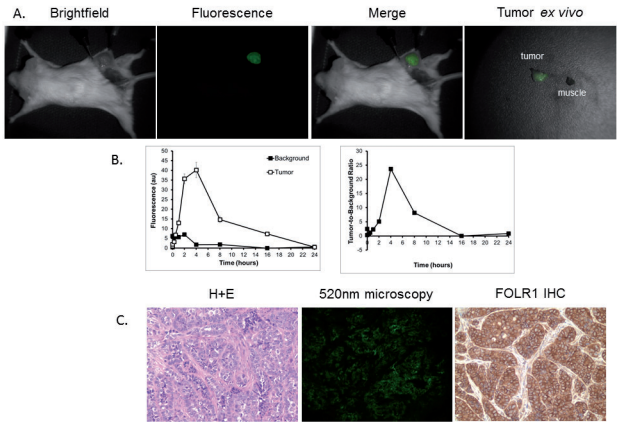

Figure 3. — *In vivo* fluorescent imaging of tumor xenografts.
A.) Folate-fluorescein can detect murine flank tumors. B) After folate-fluoresce in injection resulted in peak tumor-to-background ratios two hours after injection. C) Flank tumors were confirmed to be FOLR1 by immunohistochemical staining and fluorescence microscopy.

Based on the uptake of cultured human ovarian cancer cell lines, the authors then examined the uptake and retention of folate-fluorescein by ovarian tumor xenografts. When tumors reached 300 mm^3, animals were injected with 0.1 mg/kg folate-fluorescein and subjected to fluorescent imaging at 520 nm (Figure 3a) at various time points. No toxicity or weight differences were observed during this study. Initially, during the first hour, the tumor and surrounding tissues were equally fluorescent. The background signal diminished rapidly over one hour. By two hours, the fluorescence from the tumor peaked, and the signal diminished to ~10% over the next eight hours and had decreased to background levels within 24 hours. Over the initial of four to six hours, the dye accumulated in the tumor and the background signal diminished substantially. The peak TBR in the primary tumor to normal tissue was at four hours (Figure 3b). At that time point, the TBR was 23.6 ± 8.7. The tumors were harvested and tissues underwent histopathologic analysis. Fluorescence microscopy at $\lambda_{excitation}$520 nm revealed the cancer cells were fluorescent (Figure 3c). To further confirm that the tracer was the source of the fluorescence on the tumor cells, the tumor cells were co-cultured with folate-fluorescein and then stained with an anti-FITC antibody. Again, this showed 1:1 correlation of fluorescence with the antibody to the fluorophore.

Next, in order to determine the value of intraoperative imaging for peritoneal cytoreduction during ovarian can-

Figure 4a

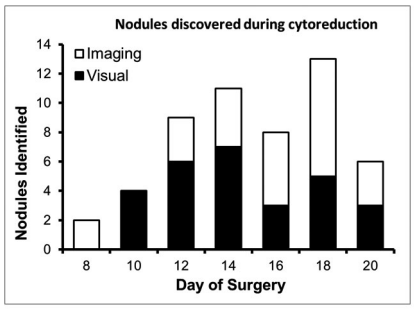

Figure 4b

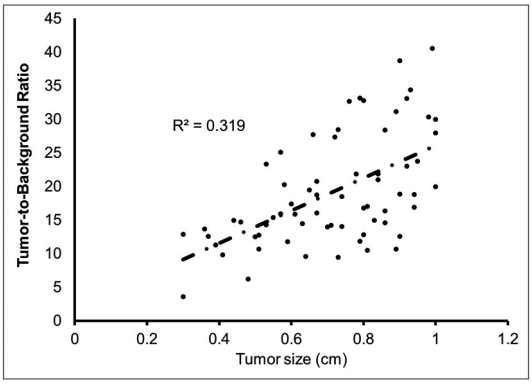

Figure 4. — Intraoperative fluorescent imaging for peritoneal cytoreduction in murine model.
A) Folate-fluorescein can detect sub-centimeter ovarian nodules. Intraoperative imaging is particularly effective at identifying peritoneal nodules early and helps to identify implants that would otherwise be difficult to detect. B) Although larger tumors were more fluorescent, there was no clear trend showing a correlation between tumor size and tumor-to-background ratio.

cer surgery, the authors utilized an intraperitoneal model of ovarian cancer. The investigators, on average, found one to three nodules on Day 7 and three to five nodules on Day 21 by unaided visual inspection (Figure 4a). Their sensitivity for identifying tumors without intraoperative imaging from Days 7 to 21 improved with increasing nodule size. The investigators incorrectly isolated eight lesions from the abdomen which ultimately were not cancer deposits. By Day 14, the surgeon, without intraoperative imaging, identified an average of seven nodules per animal (range 0-12), whereas the surgeon could identify a mean of 11 nodules (range 0-18, $p < 0.03$) by intraoperative imaging. Thus, in triplicate experiments, the addition of the intraoperative imaging, the investigators located one to five more nodules per mouse (mean 3.8, $p < 0.01$). There were no false positive nodules removed by intraoperative imaging. The smallest nodule detected by the investigators was 5 mm, however, with the addition of imaging, the smallest nodule was 2 mm. The authors discovered that the most valuable use of intraoperative imaging was during Days 5 to 8. Using visual inspection alone, they could not identify any nodules during the first week of implantation. However, imaging routinely identified one (34%) to two (16%) nodules during the initial week at various time points. Routine H&E confirmed these microscopic foci.

Figure 5

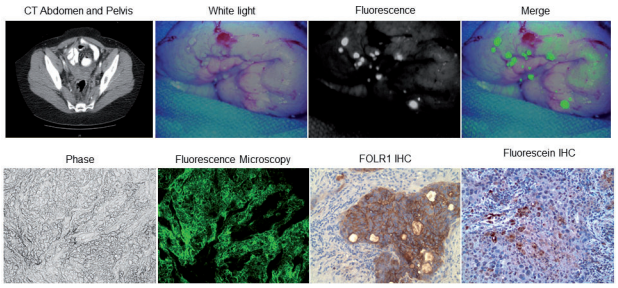

Figure 5. — Intraoperative fluorescent imaging reveals extensive disease in a human.
Folate-fluorescein based intraoperative fluorescence imaging can identify human ovarian cancer implants in the peritoneum. In this pilot study, multiple peritoneal implants are visible. Fluorescence microscopy confirmed cellular localization of folate-FITC to cancer cells, which were FRα+ and anti-FITC+.

Next, the authors analyzed the TBR to tumor size for each nodule. Using their standard digital imaging system, they found no correlation of tumor size (range 2–10 mm) and TBR (0.6–48.2) of true positive tumor implants (Figure 4b). They observed that small variations in tumor size were not markedly different in fluorescence. There was a trend towards larger nodules demonstrating greater fluorescence, however, this did not reach statistical significance.

Based on these preclinical findings, the authors conducted a pilot study on five human patients with a known diagnosis of ovarian carcinoma. All five patients had serous ovarian carcinoma, the average age of the patients was 58.8 years (38-70), and they were diagnosed with Stage IIC-IV disease. Extra tumor nodules were found in two patients (two and three nodules, respectively), while no extra tumor was identified after intraoperative imaging in another two patients. The fifth patient had extensive intraperitoneal disease identified. This patient was a 38-year-old G2P2002 with recurrent Stage IV ovarian cancer status post total abdominal hysterectomy with bilateral salpingo-oophorectomy with suboptimal debulking followed by four lines of different chemotherapies. She underwent secondary debulking with fluorescent folate dye with intraoperative investigation. Intraoperative imaging with fluorescent dye revealed extensive disease (Figure 5), which was significantly more extensive than identified on standard preoper-

ative imaging (CT scan). Preoperative imaging showed only four tumor nodules (a 14×10-mm inter-aortocaval lymph node, a 15×9-mm lymph node anterior to the right psoas, a 17×13-mm lymph node in the right external iliac region, and an ill-defined soft tissue prominence anterolateral to the sigmoid and posterior to the urinary bladder). No adverse events or toxicity associated with the study drug were noted in the five study patients. The mean TBR was 6.3 ± 4.9 with no false positive nodules harvested. Fluorescence microscopy confirmed tumor cell localization of FITC and final pathology confirmed the tumors to be serous ovarian carcinomas.

Discussion

In this translational project, the authors confirmed that human ovarian adenocarcinomas upregulated levels of the FRα. They tested a number of ovarian tumor cells lines and found two that grew folate receptor positive flank tumors. They then showed that their folate-fluorescein contrast agent was able to localize to these tumors. Furthermore, they showed that for the detection of residual disease after surgical resection, fluorescent imaging was superior to visual inspection and manual palpation in a murine model. They believe this methodology is practical and feasible for gynecologic oncologists. The use of a visible wavelength fluorophore avoids ionizing radiation and confers no risk to the patient, surgeon or operating room personnel. Optical imaging is easily understood by surgeons with no need for special training to interpret or process the data.

The present authors found no correlation of tumor size and TBR in the murine tumor models. Whether this accurately reflects the human scenario is unclear due to the relatively homogeneity of tumor histology in their murine models. In other studies, they found that human tumors that have higher cellular content and less fibroblasts, necrosis and mucinous composition tend to be more fluorescent in comparison to less cellular cancer nodules of equal size [19]. To their knowledge, no group has examined the FRα expression level per individual cancer cell in various histological subtypes of ovarian adenocarcinomas. Another challenge of measuring TBR of ovarian tumors is the technical factors in obtaining data in the peritoneum. Due to the natural variations of the peritoneal cavity, there are significant differences in the nodule distance from the lens of the imaging device, which are likely to cause a variation in the data that cannot be accounted for by measuring the background signal.

This study was limited by a number of factors. First, in the present murine model, the authors used tumor recurrence as a surrogate for residual disease after surgical resection. Though this is a logical conclusion, it is only validated by extrapolation of results from previous work performed in this lab. Secondly, the visual inspection and manual palpation of resection beds was performed by non-surgeon investigators, thus, their ability to detect suspicious residual disease is unknown. However, both practitioners were very experienced in murine surgical techniques. Lastly, the strength of this data could be improved by randomizing mice to traditional resection *vs.* fluorescence aided resection rather than performing both on the same cohort.

The implications of tumor fluorescence imaging are far-reaching. The value of this technology is to draw attention to tissues that would otherwise not have been examined. This improves intraoperative staging and removal of residual disease. Cytoreductive surgery may become more accurate for many cancers such as ovarian carcinoma, sarcomas, and malignant mesothelioma. In patients with prior surgery and/or radiation-induced injury, tumor fluorescence could identify cancer deposits in a "hostile" surgical field, where the normal visual and tactile cues may be missing or confounding. Furthermore, for minimally invasive and robotic operations, laparoscopies, colonoscopies and esophagoscopies, where the surgeon has no benefit of manual palpation, tumor fluorescence may improve identification of tumor deposits. Finally, as the full capabilities of this approach are understood, the "real-time" aspects of tumor fluorescence imaging may provide surgeons with a tool to improve decision making in the operating room in a very rapid and cost-efficient manner.

Acknowledgements

Grant Support: This work was supported by the "Be The Difference Foundation" and The National Institutes of Health Transformative R01 CA193556.

References

[1] Siegel R.L., Miller K.D., Jemal A.: "Cancer statistics, 2016". *CA. Cancer J. Clin.,* 2016, *66*, 7.

[2] Chang S.J., Bristow R.E., Ryu H.S.: "Impact of complete cytoreduction leaving no gross residual disease associated with radical cytoreductive surgical procedures on survival in advanced ovarian cancer". *Ann. Surg. Oncol,.* 2012, *19*, 4059.

[3] Holt D., Okusanya O., Judy R., Venegas O., Jiang J., DeJesus E., *et al.*: "Intraoperative near-infrared imaging can distinguish cancer from normal tissue but not inflammation". *PLoS One,* 2014, *9*, 103342.

[4] Madajewski B., Judy B.F., Mouchli A., Kapoor V., Holt D., Wang M.D., *et al.*: "Intraoperative near-infrared imaging of surgical wounds after tumor resections can detect residual disease". *Clin. Cancer Res.,* 2012, *18*, 5741.

[5] Okusanya O.T., Holt D., Heitjan D., Deshpande C., Venegas O., Jiang J., *et al.*: "Intraoperative near-infrared imaging can identify pulmonary nodules". *Ann Thorac Surg.*, 2014, 98, 1223.

[6] Okusanya O.T., Madajewski B., Segal E., Judy B.F., Venegas O.G., Judy R.P., *et al.*: "Small portable interchangeable imager of fluorescence for fluorescence guided surgery and research". *Technol. Cancer Res. Treat*., 2015, *14*, 213.

[7] Singhal S., Nie S., Wang M.D.: "Nanotechnology applications in surgical oncology". *Annu. Rev. Med.,* 2010, *61*, 359.

[8] van Dam G.M., Themelis G., Crane L.M., Harlaar N.J., Pleijhuis R.G., Kelder W., *et al.*: "Intraoperative tumor-specific fluorescence imaging in ovarian cancer by folate receptor-alpha targeting: first in-human results". *Nat. Med.,* 2011, *17*, 1315.

[9] Basal E., Eghbali-Fatourechi G.Z., Kalli K.R., Hartmann L.C., Goodman K.M., Goode E.L., *et al.*: "Functional folate receptor alpha is elevated in the blood of ovarian cancer patients". *PLoS One*, 2009, *4*, e6292.

[10] Leung F., Dimitromanolakis A., Kobayashi H., Diamandis E.P., Kulasingam V.: "Folate-receptor 1 (FOLR1) protein is elevated in the serum of ovarian cancer patients". *Clin. Biochem.,* 2013, *46*, 1462.

[11] O'Shannessy D.J., Somers E.B., Palmer L.M., Thiel R.P., Oberoi P., Heath R., *et al.*: "Serum folate receptor alpha, mesothelin and megakaryocyte potentiating factor in ovarian cancer: association to disease stage and grade and comparison to CA125 and HE4". *J. Ovarian Res.,* 2013, *6*, 29.

[12] Crane L.M., Arts H.J., van Oosten M., Low P.S., van der Zee A.G., van Dam G.M., *et al.*: "The effect of chemotherapy on expression of folate receptor-alpha in ovarian cancer". *Cell. Oncol. (Dordr).,* 2012, *35*, 9.

[13] Mantovani L.T., Miotti S., Menard S., Canevari S., Raspagliesi F., Bottini C., *et al.*: "Folate binding protein distribution in normal tissues and biological fluids from ovarian carcinoma patients as detected by the monoclonal antibodies MOv18 and MOv19". *Eur. J. Cancer,* 1994, *30A*, 363.

[14] Kalli K.R., Oberg A.L., Keeney G.L., Christianson T.J., Low P.S., Knutson K.L., *et al.*: "Folate receptor alpha as a tumor target in epithelial ovarian cancer". *Gynecol. Oncol.,* 2008, *108*, 619.

[15] Kelemen L.E., Sellers T.A., Keeney G.L., Lingle W.L.: "Multivitamin and alcohol intake and folate receptor alpha expression in ovarian cancer". *Cancer Epidemiol. Biomarkers Prev.,* 2005, *14*, 2168.

[16] Benard J., Da Silva J., De Blois M.C., Boyer P., Duvillard P., Chiric E., *et al.*: "Characterization of a human ovarian adenocarcinoma line, IGROV1, in tissue culture and in nude mice". *Cancer Res.,* 1985, 45,4970.

[17] Predina J.D., Judy B., Fridlender Z.G., Aliperti L.A., Madajewski B., Kapoor V., *et al.*: "A positive-margin resection model recreates the postsurgical tumor microenvironment and is a reliable model for adjuvant therapy evaluation". *Cancer Biol. Ther.,* 2012, *13*, 745.

[18] Elnakat H., Ratnam M.: Role of folate receptor genes in reproduction and related cancers. *Front. Biosci.,* 2006, 11,506.

[19] Judy R.P., Keating J.J., DeJesus E.M., Jiang J.X., Okusanya O.T., Nie S., *et al.*: "Quantiication of tumor fluorescence during intraoperative optical cancer imaging". *Sci. Rep.*, 2016, *5*, 16208.

Corresponding Author:
J.L. TANYI, M.D., PHD
University of Pennsylvania School of Medicine
3400 Spruce Street
Philadelphia, PA 19104 (USA)
e-mail: janos.tanyi@uphs.upenn.edu